Spatially resolved biosensing with a molded plasmonic crystal

Viktor Malyarchuk[a)]
Department of Materials Science and Engineering, University of Illinois at Urbana-Champaign, Urbana, Illinois 61801

Matthew E. Stewart
Department of Chemistry, University of Illinois at Urbana-Champaign, Urbana, Illinois 61801

Ralph G. Nuzzo and John A. Rogers[b)]
Department of Materials Science and Engineering, University of Illinois at Urbana-Champaign, Urbana, Illinois 61801 and Department of Chemistry, University of Illinois at Urbana-Champaign, Urbana, Illinois 61801

(Received 11 February 2007; accepted 25 April 2007; published online 18 May 2007)

The authors report the use of a type of quasi-three-dimensional plasmonic crystal for spatially resolved detection of biochemical binding events, with a spatial resolution of tens of microns and submonolayer binding sensitivity. In demonstration experiments, fibrinogen patterns nonspecifically adsorbed to the crystal surface were spatially and spectroscopically resolved using monochromatic and white light illumination. The experimental simplicity of the fabrication and use of these sensors, their compact form factors together with the high detection sensitivities and spatial resolution that can be achieved, collectively make these devices interesting as candidates for label-free array-based bioanalytical detection. © *2007 American Institute of Physics*. [DOI: 10.1063/1.2740591]

Continuous, flat metal film based surface plasmon resonance sensors dominate the area of label-free biological/chemical detection.[1] The popularity of these systems derives from their ability to measure small changes in refractive index at surfaces, which has proven invaluable for research in various fields of natural science. Instruments that use such sensors typically incorporate prisms to couple light into and out of a single surface plasmon polarition (SPP) mode that propagates at the interface between the metal (typically ~50 nm of gold) and the surrounding dielectric medium. In addition to basic sensing, these systems can be used to image binding events in two dimensions through implementation of array or charge coupled detectors.[2,3] A disadvantage, which can have important practical consequences, is that the prism based coupling involves cumbersome optics that are difficult to integrate into portable, low-cost devices for rapid bioanalytical measurements in well plates, arrays, or integrated microfluidic devices.[4,5]

These limitations can be avoided by replacing the prisms with grating based coupling schemes such as those that use periodic relief structures or arrays of nanoholes.[6–9] Such structures can be used for chemical sensing/biosensing by exploiting the interaction either of localized or propagating SPPs with the surrounding media.[10] Recent studies of quasi-three-dimensional (3D) plasmonic crystals that consist of arrays of nanoholes coupled to underlying disks demonstrate that multiple, well-defined localized, as well as propagating resonances can occur in these systems.[11] Finite difference time domain calculations can quantitatively reproduce all of associated features that appear in the spectral properties of normal incidence transmission through these crystals, thereby enabling their use in a type of multispectral operation in which information from all of the spectral features is used to enable high sensitivity. This letter demonstrates the use of these quasi-3D plasmonic crystals in a fully two dimensional spatial imaging mode for which micron resolution and submonolayer sensitivities are simultaneously possible. Single wavelength and integrated multispectral imaging results are presented and compared to one another and to previous results obtained in a much simpler one-dimensional (1D) imaging mode.[11] These results, together with the simple procedures used to fabricate the crystals, may be important for a range of applications in chemical sensing/biosensing and imaging where low cost, compact form factor, and high performance are important.

Figures 1(a) and 1(b) illustrate the geometry of the crystals and the optical setup used to operate them in a transmission imaging mode. The crystal consists of a polymer layer molded into a structure that consists of a square array of cylindrical depressions with diameters, depths, and periodicity of 480, 350, and 780 nm, respectively, by the use of a soft imprint lithographic method.[10] Uniformly coating this embossed polymer layer using a directional flux of Au from an electron beam evaporator creates a planar layer (~50 nm) of Au with circular holes and an array of Au disks at the bottoms of the cylindrical wells. The electromagnetic coupling between the two levels in this quasi-3D structure influences the optical properties. Figure 1(b) presents a scanning electron micrograph of a typical sample, which covers an area of 16 mm^2. The ability of this soft imprint technique to fabricate easily large area crystals with excellent spatial uniformity in the dimensions is important for imaging applications like those described here and, ultimately, for low cost (and possibly disposable) implementations. For operation in an imaging mode, light from an air cooled 150 W tungsten halogen lamp passes through a Czerny-Turner monochromator and the collimated output shines through the crystal. Collecting optics create an ~3× magnified image of the sample on the InGaAs based focal plane array (320 × 256 pixels each of which is 30 × 30 μm) of an XEVA-

a)Electronic mail: malyarchuk@mrl.uiuc.edu
b)Author to whom correspondence should be addressed; electronic mail: jrogers@uiuc.edu

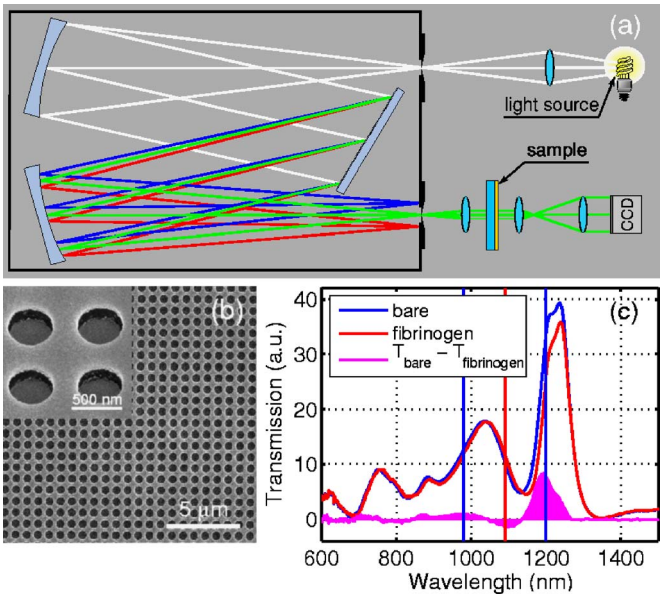

FIG. 1. (a) Optical setup used for spatial imaging using a molded plasmonic crystal sensor and (b) scanning electron micrograph of a typical plasmonic crystal. The inset shows a higher magnification tilted micrograph. Metal disks at the bottom of the nanowells are clearly visible. (c) Transmission spectra of the regions of the crystal coated (red) with fibrinogen and bare regions (blue) both evaluated in air. The difference between these spectra are shown in pink. The vertical lines show spectral positions of maximum sensitivity/contrast: (blue) bare areas show greater transmission and (red) fibrinogen coated areas show greater transmission.

FPA-1.7-320 infrared camera (XenICs, Belgium). Taking into account magnification by collection optics, the resolution of this particular imaging system is ~10 μm. A three-stage thermoelectric cooling element maintains the operating temperature of the camera at 210 K. This low temperature mode not only improves the signal to noise ratio but also provides better than 2.5% linearity over the dynamic range of the camera.

The imaging experiments used crystals coated with a pattern of ultrathin layers of fibrinogen. A removable microfluidic device provided the means to achieve this patterned deposition.[11] This process involves flowing fibrinogen from bovine plasma (Sigma) in a phosphate buffered saline (PBS) (Bio Whittaker) through microfluidic channels formed by conformal contact of an embossed piece of poly(dimethylsiloxane) (PDMS) with the surface of the crystal. Rinsing the channels with PBS, removing the PDMS, rinsing the entire plasmonic crystal thoroughly with PBS and then drying it under stream of nitrogen completes the patterning process.[12] A crystal processed in this manner, for the geometries studied here, supports five 250 μm wide lines of nonspecifically adsorbed fibrinogen, each separated by 250 μm.

To identify the wavelengths that provide the highest imaging contrast, we acquired transmission spectra from fibrinogen patterned and unpatterned (bare) regions of the sample using a Fourier transform infrared spectrometer (Bruker Vertex 70, globar lamp) combined with an infrared microscope (Bruker Hyperion 2000 and a liquid-nitrogen-cooled InSb detector). Figure 1(c) shows microtransmission spectra in the uncoated and coated regions of a typical crystal and the differences between these spectra. Overall, the adsorption of fibrinogen increases the refractive index at the surface of the crystal, resulting in a slight redshift (and change in transmission) of some of the resonant features in

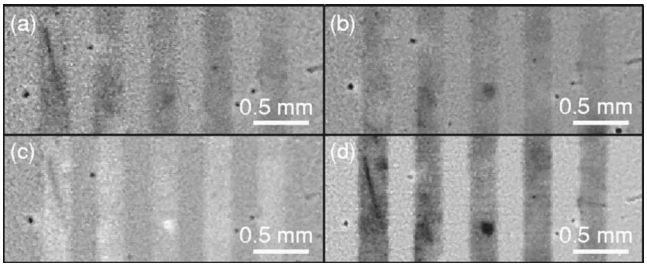

FIG. 2. Spatial imaging with a plasmonic crystal sensor, using white light and selected wavelengths: (a) white light, (b) 980 nm, (c) 1090 nm, and (d) 1200 nm. The images are background corrected.

the transmission spectra. The wavelength dependent sensitivities revealed by these measurements provide a means to understand the contrast observed in imaging. The quantitative analysis of spectra of this type, the sensitivity that can be achieved, and other features of this system can be found elsewhere.[11]

Figure 2 shows two-dimensional images of the fibrinogen patterns on the surface of the plasmonic crystal, as collected using the setup illustrated in Fig. 1 and described above.

This series of images used either monochromatic illumination, at various wavelengths, or broadband white light. The wavelengths correspond to those that exhibit peaks in sensitivity, as determined by the results of Fig. 1(c). The blue and red lines correspond to wavelengths for which the contrast in the images corresponds to larger or smaller transmission in the uncoated and fibrinogen coated regions of the sample, respectively. In particular, for illumination at 1090 nm, the regions of the crystal coated with fibrinogen appear brighter than the uncoated regions, because the coating increases the transmission at this wavelength. By contrast, the fibrinogen coated regions appear darker than the uncoated regions at 980 and 1200 nm, because the coating decreases the transmission at these wavelengths. The image obtained using white light illumination shows dark regions at the locations of the fibrinogen, because the total decrease in transmission is larger than the total increase in transmission, in a multispectral sense convolved over the response of the camera in the spectral range investigated. This ability to perform imaging with white light is important because it eliminates entirely the need for the monochromator or for wavelength bandpass filter elements. Imaging of this type of structure is possible due to the extremely high binding sensitivity of the molded plasmonic crystals, as quantitatively described elsewhere in 1D imaging modes.[11]

Raw images obtained directly from the camera had smooth variations in brightness that result from the intensity profile of the illuminating light. To eliminate these effects, the images were divided by the background, as determined by removing the sample from the optical path and recording an image of the illuminating light. In such background corrected images, the numerical value at every pixel corresponds to the actual transmission value. Such images are shown in Fig. 2.

Figure 3 shows intensity profiles obtained by calculating the average intensity for each column of pixels in the background corrected images.

Analysis of the step edges at the fibrinogen patterned and unpatterned regions of the crystal was performed by convolving a step function and a Gaussian with a σ=20 μm.

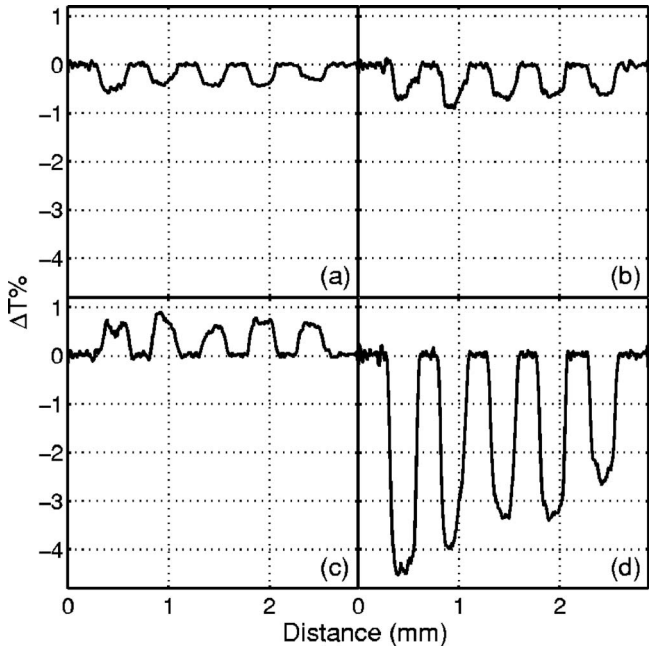

FIG. 3. Integrated profiles of spatial images collected with a plasmonic crystal sensor, using white light and selected wavelengths: (a) white light, (b) 980 nm, (c) 1090 nm, and (d) 1200 nm.

This characteristic width is comparable to the resolution of the imaging optics (1 pixel $\sim 10\ \mu$m).

Effective thicknesses for the fibrinogen coating can be determined by using approximate calibration constants obtained from the second analogous sensor integrated into the fluid cell. Sequential injections of aqueous solutions of polyethylene glycol determined the optical response as a function of change in refractive index. We found that such calibration data, when used in a spectrally integrated mode, can be applied to the white light illuminated image (Fig. 2) to yield effective thicknesses of 8 ± 1 nm, in agreement with expectation.[11]

The overall uniformity of the samples, as defined by the processing conditions used to form them, is important for these types of imaging experiments. To evaluate uniformity, we performed statistical analysis of the transmission signals by examining the six spatially separated protein-free stripes in the images in Fig. 2. The transmission values at all pixels in each of these regions were fitted with normal distribution functions. The averages determined from these distributions change by less than 0.1% from stripe to stripe across the imaged area. Within a given area, the standard deviations are $\sim 1\%$, which is significantly smaller than the difference in average transmission between the coated and uncoated regions. These results indicate that the fabrication methods provide extremely high levels of spatial uniformity in large area samples, thereby satisfying a key technical challenge for imaging based plasmonic crystal sensors. Most of the defects visible in images are likely nontransparent contamination on the sample surface. They are always darker than the surrounding area. There are also some spots that show areas with higher protein thickness. They show stronger response and appear brighter or darker than the other areas, depending on wavelength.

In conclusion, this letter demonstrates the use of plasmonic crystals for imaging based biosensing with good spatial resolution and high sensitivity, in both monochromatic and white light illumination conditions. The simplicity of the experimental setups and the compact form factor associated with the crystals and the imaging systems represent key advantages of this approach. The use of incoherent light and fast acquisition speed (200 ms averaging time was used here; 10 ms is the frame rate limit of the camera) makes it also a suitable tool for imaging of dynamic events. The data show, furthermore, that one of the best optical detection modes is also the simplest: only a white light source, a plasmonic crystal sensor, and basic imaging optics are needed. The ability to perform such measurements without a laser or a spectrometer makes the system easy to miniaturize, cheap to construct, and straightforward to implement.

The authors acknowledge the support of the U.S. Department of Energy (DEFG02-91-ER45439). All measurements reported here were carried out in the Center for Microanalysis of Materials, University of Illinois, which is partially supported by the U.S. Department of Energy under Grant No. DEFG02-91-ER45439.

[1] J. Homola, Anal. Bioanal. Chem. **377**, 528 (2003).
[2] E. Fu, J. Foley, and P. Yager, Rev. Sci. Instrum. **74**, 3182 (2003).
[3] G. Steiner, Anal. Bioanal. Chem. **379**, 328 (2004).
[4] J. M. Brockman, B. P. Nelson, and R. M. Corn, Annu. Rev. Phys. Chem. **51**, 41 (2000).
[5] J. S. Shumaker-Parry, R. Aebersold, and C. T. Campbell, Anal. Chem. **76**, 2071 (2004).
[6] W. Ebbesen, H. J. Lezec, H. F. Ghaemi, T. Thio, and P. A. Wolff, Nature (London) **391**, 667 (1998).
[7] S. C. Hohng, Y. C. Yoon, D. S. Kim, V. Malyarchuk, R. Müller, C. Lienau, J. W. Park, K. H. Yoo, J. Kim, H. Y. Ryu, and Q. H. Park, Appl. Phys. Lett. **81**, 3239 (2002).
[8] D. S. Kim, S. C. Hohng, V. Malyarchuk, Y. C. Yoon, Y. H. Ahn, K. J. Yee, J. Park, J. Kim, Q. H. Park, and C. Lienau, Phys. Rev. Lett. **91**, 143901 (2003).
[9] W. L. Barnes, W. A. Murray, J. Dintinger, E. Devaux, and T. Ebbesen, Phys. Rev. Lett. **92**, 107401 (2004).
[10] V. Malyarchuk, F. Hua, N. H. Mack, V. T. Velasquez, J. O. White, R. G. Nuzzo, and J. A. Rogers, Opt. Express **13**, 5669 (2005).
[11] M. E. Stewart, N. H. Mack, V. Malyarchuk, J. A. N. T. Soares, T.-W. Lee, S. K. Gray, R. G. Nuzzo, and J. A. Rogers, Proc. Natl. Acad. Sci. U.S.A. **103**, 17143 (2006).
[12] J. Monahan, A. A. Gewirth, and R. G. Nuzzo, Anal. Chem. **73**, 3193 (2001).